Am J Physiol Cell Physiol
279: C375–C382, 2000.

Forskolin-induced apical membrane insertion of virally expressed, epitope-tagged CFTR in polarized MDCK cells

MARYBETH HOWARD,[1] XIAOSUI JIANG,[1] DONNA BEER STOLZ,[2] WARREN G. HILL,[2] JENNIFER A. JOHNSON,[1] SIMON C. WATKINS,[2] RAYMOND A. FRIZZELL,[2] CHRISTINA M. BRUTON,[3] PAUL D. ROBBINS,[3] AND ORA A. WEISZ[1]
Laboratory of Epithelial Cell Biology, Renal-Electrolyte Division, Departments of [1]Medicine, [2]Cell Biology and Physiology, and [3]Molecular Genetics and Biochemistry, University of Pittsburgh, Pittsburgh, Pennsylvania 15213-2500

Received 13 July 1999; accepted in final form 14 February 2000

Howard, Marybeth, Xiaosui Jiang, Donna Beer Stolz, Warren G. Hill, Jennifer A. Johnson, Simon C. Watkins, Raymond A. Frizzell, Christina M. Bruton, Paul D. Robbins,and Ora A. Weisz. Forskolin-induced apical membrane insertion of virally expressed, epitope-tagged CFTR in polarized MDCK cells. *Am J Physiol Cell Physiol* 279: C375–C382, 2000.—Channel gating of the cystic fibrosis transmembrane conductance regulator (CFTR) is activated in response to cAMP stimulation. In addition, CFTR activation may also involve rapid insertion of a subapical pool of CFTR into the plasma membrane (PM). However, this issue has been controversial, in part because of the difficulty in distinguishing cell surface vs. intracellular CFTR. Recently, a fully functional, epitope-tagged form of CFTR (M2–901/CFTR) that can be detected immunologically in nonpermeabilized cells was characterized (Howard M, Duvall MD, Devor DC, Dong J-Y, Henze K, and Frizzell RA. *Am J Physiol Cell Physiol* 269: C1565–C1576, 1995; and Schultz BD, Takahashi A, Liu C, Frizzell RA, and Howard M. *Am J Physiol Cell Physiol* 273: C2080–C2089, 1997). We have developed replication-defective recombinant adenoviruses that express M2–901/CFTR and used them to probe cell surface CFTR in forskolin (FSK)-stimulated polarized Madin-Darby canine kidney (MDCK) cells. Virally expressed M2–901/CFTR was functional and was readily detected on the apical surface of FSK-stimulated polarized MDCK cells. Interestingly, at low multiplicity of infection, we observed FSK-stimulated insertion of M2901/CFTR into the apical PM, whereas at higher M2–901/CFTR expression levels, no increase in surface expression was detected using indirect immunofluorescence. Immunoelectron microscopy of unstimulated and FSK-stimulated cells confirmed the M2–901/CFTR redistribution to the PM upon FSK stimulation and demonstrates that the apically inserted M2–901/CFTR originates from a population of subapical vesicles. Our observations may reconcile previous conflicting reports regarding the effect of cAMP stimulation on CFTR trafficking.

cystic fibrosis; cystic fibrosis transmembrane conductance regulator; epithelia; adenovirus; Madin-Darby canine kidney; protein traffic

IN MEMBRANE PATCHES AND LIPID BILAYERS, cAMP/protein kinase A-mediated activation of the cystic fibrosis transmembrane conductance regulator (CFTR) results in increased open channel probability. Other experiments using intact cells are consistent with cAMP-mediated insertion of a submembranous pool of CFTR into the apical membrane. The involvement of protein kinase A in regulation of channel gating vs. membrane insertion has been controversial. Takahashi et al. (35) have demonstrated that cAMP stimulation causes an increase in capacitance and membrane surface area of *Xenopus* oocytes expressing wild-type CFTR. Schwiebert et al. (32) also found that cAMP stimulation results in exocytosis of CFTR in airway epithelial cells. By contrast, Moyer et al. (23) recently concluded, using green fluorescent protein (GFP)-tagged CFTR, that CFTR expression at the apical surface of Madin-Darby canine kidney (MDCK) type I cells is unaltered by channel stimulation. This group also used confocal microscopy to conclude that cAMP stimulation of the airway epithelial cell line Calu-3 did not cause CFTR redistribution (19). To further investigate this issue, we generated a replication-defective recombinant adenovirus expressing CFTR that has been epitope tagged on an extracellular loop (AV-M2–901; see Refs. 13 and 31) and used this virus to study trafficking of CFTR in polarized epithelial cells. Unlike the GFP-tagged CFTR, this epitope-tagged construct has been extensively characterized and is known to be fully functional (31). An additional advantage of this construct is the extracellular positioning of the epitope, which allows immunofluorescence-based detection of cell surface CFTR in intact cells. Finally, because we can control the amount of virus used to infect the cells, our system allows us to examine the effect of protein expression level on regulated membrane insertion.

EXPERIMENTAL PROCEDURES

Cell lines. Low-passage MDCK cells (type II, Heidelberg clone) were maintained in modified Eagle's medium (Cellgro; Fisher Scientific, Pittsburgh, PA) supplemented with 10% FBS (Atlanta Biologicals, Norcross, GA), penicillin (100

Address for reprint requests and other correspondence: O. A. Weisz, Renal-Electrolyte Division, Univ. of Pittsburgh, 3550 Terrace St., Pittsburgh, PA 15261 (E-mail: weisz@msx.dept-med.pitt.edu).

The costs of publication of this article were defrayed in part by the payment of page charges. The article must therefore be hereby marked "*advertisement*" in accordance with 18 U.S.C. Section 1734 solely to indicate this fact.

 0363-6143/00 $5.00 Copyright © 2000 the American Physiological Society

U/ml), and streptomycin (100 μg/ml). Some experiments were performed using MDCK II CCL cells (originally from American Type Culture Collection, Rockville, MD) maintained in DMEM-F-2 (GIBCO BRL, Gaithersburg, MD) supplemented with 10% FBS; similar results were obtained with both cell lines. Cells were seeded at high density (~5×10^5 cells/well) in 12-mm transwells (0.4 μm pore; Costar, Cambridge, MA) and were infected with recombinant adenovirus 2–3 days postplating (Heidelberg clone) or 5 days postplating (CCL cells). Experiments were performed the following day, unless otherwise noted. For fluorescence measurements of anion permeability using 6-methoxy-*N*-(3-sulfopropyl)quinolinium (SPQ), ~5×10^5 MDCK cells were plated on 25-mm coverslips in 35-mm dishes and allowed to grow for 2–3 days before infection.

Generation of recombinant adenoviruses. M2–901/CFTR was subcloned into the pAdlox vector behind the cytomegalovirus promoter (10). An E1- to E3-deleted recombinant adenovirus encoding M2–901/CFTR (AV-M2–901) was generated by cotransfection of the pAdlox M2–901/CFTR and ψ5 DNA into CRE8 cells using the method described by Hardy et al. (10) and was purified as described by Henkel et al. (11). Viral titer was estimated by measuring the optical density at 260 nm of the final preparation and was between 10^{12} and 10^{13} particles/ml. Viruses were stored in small aliquots to avoid repeated freeze-thaw cycles. AV-CFTR was a gift from Genzyme (via Joseph Pilewski).

Adenoviral infection. Filter-grown MDCK cells were washed by adding 3 ml of calcium-free PBS containing 1 mM $MgCl_2$ (PBS-M) to the apical chamber and allowing it to spill over into the basolateral compartment. After 3–5 min at room temperature, the PBS-M was removed, and 150 μl of PBS-M containing recombinant adenovirus was added to the apical compartment. The medium in the basolateral compartment was replaced with 0.5 ml of PBS-M. The dishes were rocked briefly and then returned to an incubator for 1–2 h. Mock-infected cells were treated identically except that virus was omitted during the incubation period. Dishes were then rinsed with 2 ml of PBS-M, and cells were incubated overnight in growth medium (1 ml apical, 1.5 ml basolateral). In most experiments, 2 mM sodium butyrate was added for 18–24 h before the start of the experiment to increase expression of M2–901/CFTR.

Radiolabeling and immunoprecipitation of M2–901/CFTR. Filter-grown MDCK cells (uninfected or infected with AV-M2–901) were starved in cysteine-free, methionine-free MEM containing 0.35 g/l $NaHCO_3$, 10 mM HEPES, and 10 mM MES, pH 7.0 (*medium A*), for 30 min and then were placed on a 25-μl drop of *medium A* containing 1 mCi/ml ^{35}S-labeled Express (NEN, Boston, MA) in a humidified chamber for 3 h at 37°C. The filters were rinsed with PBS, and cells were solubilized for 1 min at 4°C in lysis buffer (1% Nonidet P-40 and 1 mM EDTA in 20 mM HEPES, pH 7) containing protease inhibitor cocktail (10 μM leupeptin, 1 μM pepstatin A, 2 μg/ml soybean trypsin inhibitor, 2 μg/ml aprotinin, 40 μg/ml phenylmethylsulfonyl fluoride, and 0.2 mM dithiothreitol). The cell lysates were precleared by incubation with normal rabbit serum at 1:20 followed by precipitation using 25 μl of protein A-Sepharose 6MB (Pharmacia Biotech, Piscataway, NJ). After centrifugation, supernatants were adjusted to 1× RIPA buffer (1% Triton X-100, 1% sodium deoxycholate, and 0.1% SDS in 50 mM Tris·HCl, pH 7.5). The samples were incubated with monoclonal antibodies against the FLAG epitope (Stratagene, La Jolla, CA) or the carboxy terminus of CFTR (Genzyme, Cambridge, MA) for 90 min, and antibody-antigen complexes were isolated using protein A-Sepharose. Samples were washed three times with RIPA buffer, and antigen-antibody complexes were eluted by incubating in electrophoresis sample buffer [125 mM Tris·HCl, pH 6.8, 5% SDS (wt/vol), and 25% (wt/vol) sucrose] containing 5% (vol/vol) 2-mercaptoethanol at 37°C for 5 min. The samples were run on a 6% SDS-PAGE gel, and the dried gel was exposed on X-ray film (X-OMAT AR; Eastman Kodak, Rochester, NY).

Western blotting of M2–901/CFTR. MDCK cells grown on six-well filter inserts were infected with AV-M2–901, as described above. Filters were induced with butyrate for 18 h before solubilization. Protein concentrations of the cell lysates were determined using the bicinchoninic acid protein assay kit (Pierce, Rockford, IL). Fifteen micrograms of protein were loaded per well and were separated through a 7.5% SDS-PAGE. Proteins were transferred to a nitrocelullose membrane and probed for CFTR protein using the following protocol. Nonspecific sites on the membrane were blocked in 10% normal goat serum-0.1% Tween 20-PBS for 1 h. The membrane was washed three times in PBS and incubated for 1 h with a CFTR R domain antibody diluted 1:1,000 in 2% BSA-0.1% Tween 20-PBS. The membrane was washed for 1 h in 0.1% Tween 20-PBS with six changes of the wash solution and was incubated with horseradish peroxidase-goat anti-rabbit antibody (1:20,000) for 1 h. The wash step was repeated, and protein was visualized using the SuperSignal kit (Pierce).

Detection of functional M2–901/CFTR using SPQ. cAMP-dependent anion efflux was monitored by SPQ (Molecular Probes, Eugene, OR) fluorescence changes in living cells as described previously (17). Subconfluent cells grown on 25-mm glass coverslips were loaded with 10 mM SPQ in hypotonic sodium iodide buffer. Iodide quenches SPQ fluorescence. Cells were mounted in a perfusion chamber placed in a heating stage set to 37°C and were perfused with buffers throughout the experiment. Imaging was performed on a Nikon Diaphot 300 inverted microscope equipped with a ×40 oil-immersion objective, image intensifier, and video camera. Excitation was at 330 nm, and image acquisition and analysis were performed using Metafluor software (Universal Imaging, West Chester, PA). The average fluorescence intensity of individual cells in a field was monitored every 15 s throughout the assay. Cells were perfused with isotonic sodium iodide buffer for 2 min, nitrate buffer for 4 min to assess the rate of iodide leakage/exchange from unstimulated cells, 4 min in nitrate buffer supplemented with 10 μM forskolin (FSK) and 200 μM IBMX (both from Calbiochem, San Diego, CA), and then 4 min in iodide buffer to requench intracellular SPQ. Functional CFTR was detected as an increase in the rate of dequenching of SPQ fluorescence upon addition of FSK/IBMX. Assays on mock-infected and adenovirus-infected cells were performed blinded.

Indirect immunofluorescence. Cells were treated (24–26 h postinfection) with or without 10 μM FSK for 20 min at 37°C and then rapidly plunged into ice-cold beakers containing PBS supplemented with 2 mM $CaCl_2$ and 1 mM $MgCl_2$ (PBS-CM). FSK (2 μM) was included in the buffer used for FSK-treated samples. Extreme care was taken during all subsequent steps to maintain the temperature of the filters at or below 4°C. The filters were then blocked with 5% normal goat serum in PBS-CM for 20 min on ice and then washed three times for 5 min each with PBS-CM. The filters were incubated with anti-FLAG antibody (1:100 dilution prepared in PBS-CM containing 3% BSA) for 1 h on ice, washed, and then incubated with Cy-3-conjugated goat anti-mouse antibody (1:1,000 dilution; Jackson ImmunoResearch Laboratories, Avondale, PA) for 1 h in the dark. After being washed, filters were fixed with 3% paraformaldehyde for 10

min on ice. In some experiments, cells were subsequently permeabilized with 0.5% Triton X-100, blocked with 0.25% ovalbumin in PBS-glycine, and incubated with a polyclonal anti-ZO-1 antibody (Zymed Laboratories, South San Francisco, CA; 1:100 dilution) followed by FITC-conjugated goat anti-rabbit antibody to visualize tight junctions.

Preembedding immunogold labeling. AV-M2–901-infected MDCK monolayers that were either FSK or mock stimulated were fixed in 2% paraformaldehyde and 0.05% glutaraldehyde in PBS (in g/l: 8 NaCl, 0.2 KCl, 1.15 $Na_2HPO_4 \cdot 7H_2O$, and 0.2 KH_2PO_4, pH 7.4) for 1 h at 4°C. Monolayers were then washed one time with PBS, two times with 0.5% BSA and 0.15% glycine in PBS (PBG buffer), and then permeabilized in 0.1% Triton X-100 in PBG for 5 min at room temperature. Monolayers were blocked in 5% normal goat serum in PBG buffer for 30 min and incubated with a 1:50 dilution of anti-carboxy terminus CFTR antibody in PBG buffer overnight at 4°C. Monolayers were washed three times for 5 min in PBG buffer at room temperature and then were incubated with 5 nm of gold conjugated to protein A (1:100; Energy Beam, Agawam, MA) for 2 h at 4°C. Monolayers were washed three times in PBG buffer and then one time in PBS before fixing immunolabeled cells in 2.5% glutaraldehyde in PBS overnight. Cells were washed three times in PBS and then postfixed in aqueous 1% osmium tetroxide and 1% Fe_6CN_3 for 1 h. Monolayers were washed three times in PBS, dehydrated through a 30–100% ethanol series, and then incubated in several changes of Polybed 812 embedding resin. The monolayers on filters were cut into strips, layered in molds, cured overnight at 37°C, and hardened for two additional days at 65°C. Ultrathin sections (60 nm) were obtained on a Riechart Ultracut E microtome and were poststained in 2% uranyl acetate in 50% methanol for 10 min and 1% lead citrate for 7 min. Sections were viewed on a JEOL JEM 1210 or 100CX transmission electron microscope at 80 kV.

Statistical analysis. Gold particles were quantitated from photographic prints taken of labeled cells. Cell surface particles were designated as gold particles within 20 nm of the cell membrane, and cell surface-to-total particle ratios per cell were determined. The mean ± SE and statistical significance using unpaired *t*-tests were obtained for these ratios using the InStat (GraphPad) statistical package.

RESULTS

MDCK cells infected with AV-M2–901 express full-length, functional CFTR at the apical surface. MDCK type II cells were mock infected or infected with AV-M2–901 or AV-CFTR as described in EXPERIMENTAL PROCEDURES. The following day, cells were metabolically labeled and then solubilized and immunoprecipitated with antibodies recognizing either the FLAG epitope or the carboxy terminus of CFTR (Fig. 1*A*). Both wild type and epitope-tagged CFTR were readily immunoprecipitated by the anti-carboxy antibody. In addition, M2–901/CFTR was also immunoprecipitated by the anti-FLAG antibody, albeit at much lower efficiency. Expression of M2–901/CFTR increased with increas-

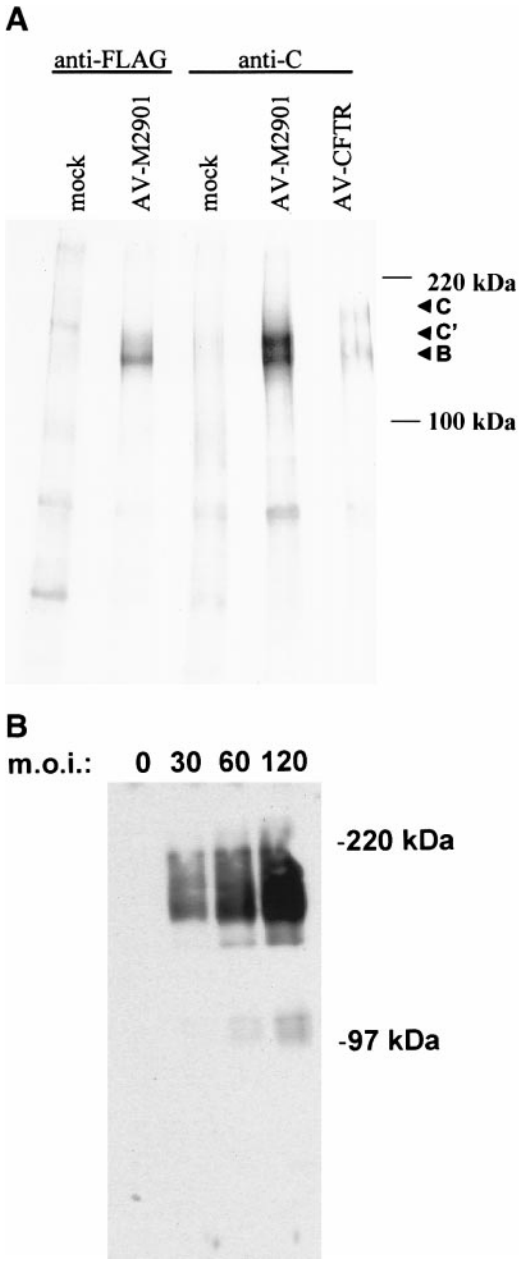

Fig. 1. *A*: immunoprecipitation of virally expressed M2–901/cystic fibrosis transmembrane conductance regulator (CFTR). Filter-grown Madin-Darby canine kidney (MDCK) cells were mock infected or infected with either adenovirus (AV)-M2–901 or AV-CFTR at a multiplicity of infection (MOI) of 50. The following day, cells were radiolabeled for 3 h with 1 mCi/ml ^{35}S-labeled Express and then rinsed with PBS and solubilized. CFTR and M2–901/CFTR were immunoprecipitated using anti-carboxy terminal antibody (anti-C) or anti-FLAG antibody as described in EXPERIMENTAL PROCEDURES. Samples were analyzed by SDS-PAGE. The core-glycosylated (B) and mature (C and C′) forms of CFTR and M2–901/CFTR, respectively, are indicated. M2–901/CFTR has only one glycosylation site; thus, the mature form of the protein (C′) migrates more rapidly than wild-type CFTR (C). Note that immunoprecipitation of M2–901/CFTR using the anti-FLAG antibody is considerably less efficient than immunoprecipitation using anti-C; this is likely due to steric interference by the extensive glycosylation near the FLAG epitope insertion site. The reduced level of wild-type CFTR expression relative to M2–901/CFTR is most likely due to decreased AV-CFTR adenovirus titer as a result of multiple freeze-thaw cycles. *B*: expression of M2–901/CFTR increases with MOI. Filter-grown MDCK cells were infected with the AV-M2–901 at the indicated MOI and induced with 2 mM sodium butyrate as described in EXPERIMENTAL PROCEDURES. Cells were lysed, and 15 μg of protein were separated by gel electrophoresis. Proteins were transferred to a nitrocellulose membrane, and CFTR was visualized using enhanced chemiluminescence.

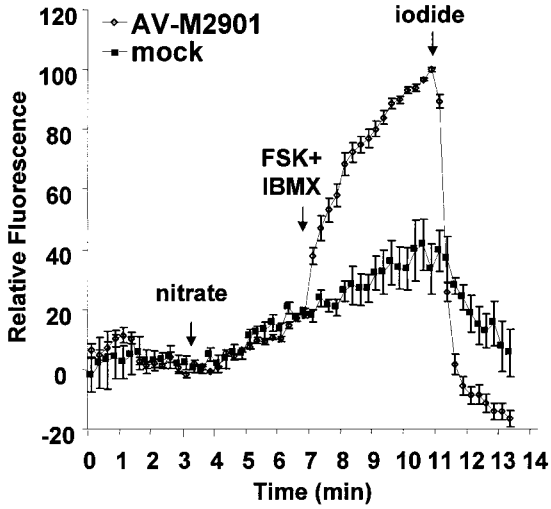

Fig. 2. Virally expressed M2–901/CFTR is functional. MDCK cells grown on glass coverslips were mock-infected or infected with AV-M2–901 at an MOI of 50. Cells were induced with 2 mM butyrate for 24 h before CFTR activity assay using 6-methoxy-*N*-(3-sulfopropyl)quinolinium (SPQ). Cells were perfused with isotonic sodium iodide buffer for 2 min, nitrate buffer for 4 min to assess the rate of iodide leakage/exchange from unstimulated cells, 4 min in nitrate buffer supplemented with forskolin (FSK) and IBMX, and then 4 min in iodide buffer to requench intracellular SPQ. The points when the perfusate reached the coverslip are noted with arrows. Functional CFTR is detected as an increase in the rate of dequenching of SPQ fluorescence upon addition of FSK and IBMX. Mock-infected cells demonstrated no cAMP-stimulated halide efflux, whereas virally infected cells showed a dramatic stimulation in SPQ dequenching in response to FSK + IBMX, indicative of halide channel activity. The traces shown represent means ± SE from 53 and 40 mock-infected and virally infected cells, respectively.

ing addition of recombinant adenovirus between a multiplicity of infection (MOI) of 30 and 120 (Fig. 1*B*).

To confirm that MDCK cells infected with AV-M2–901 expressed functional CFTR, we performed iodide efflux assays using the halide-sensitive fluorophore SPQ on mock-infected and infected cells grown on glass coverslips (Fig. 2). This assay measures halide efflux via CFTR; however, it cannot discriminate between FSK-stimulated insertion of submembranous CFTR and activation of preexisting CFTR at the plasma membrane (PM) of stimulated cells. By contrast to mock-infected cells, MDCK cells expressing M2–901/CFTR showed dramatically elevated iodide efflux in response to cAMP stimulation. Double-label indirect immunofluorescence of polarized MDCK cells infected with AV-M2–901 and stimulated with FSK demonstrated that the protein was found on the apical PM, as expected (Fig. 3). At MOI 50, we could typically detect M2–901/CFTR in ~50–80% of the cells on the filter after FSK stimulation. No effects of adenoviral infection on cell morphology, polarity, or function were observed, even when cells were infected at extremely high MOI (up to 2,500).

FSK-dependent insertion of CFTR at the PM is expression-level dependent. To investigate whether expression of M2–901/CFTR at the apical surface of MDCK cells was stimulated upon FSK addition, we infected cells with increasing MOI of AV-M2–901 and then mock-treated or FSK-treated the cells before rapid cooling and cell staining using anti-FLAG antibody (Fig. 4). No staining was evident on the cell surface of unstimulated or FSK-stimulated mock-infected cells (MOI 0). In cells infected at low MOI (30–50), there was little or no staining of M2–901/CFTR on the PM of unstimulated cells, whereas large amounts of M2–901/CFTR were found on the PM of cells infected at higher MOI (>100). Upon FSK stimulation, there was a dramatic increase in cell surface M2–901/CFTR in cells infected at low MOI, but no increase in cell surface M2–901/CFTR could be detected in cells infected at higher MOI. The range of MOI for which we could detect a difference in surface expression in FSK-stimulated vs. unstimulated cells using this method varied between experiments from 25 to 50. This is probably due to experiment-to-experiment variation in infection efficiency and to error in estimating virus titer between different batches of AV-M2–901. We never detected FSK-stimulated insertion of M2–901/CFTR in cells infected at MOI >100. However, at low MOI (30–50), we occasionally observed a few cells with considerable surface M2–901/CFTR expression in unstimulated samples; these could be cells that were infected with a high number of virus particles.

To further examine this phenomenon and to localize intracellular M2–901/CFTR, we performed immunoelectron microscopy of mock- and FSK-stimulated po-

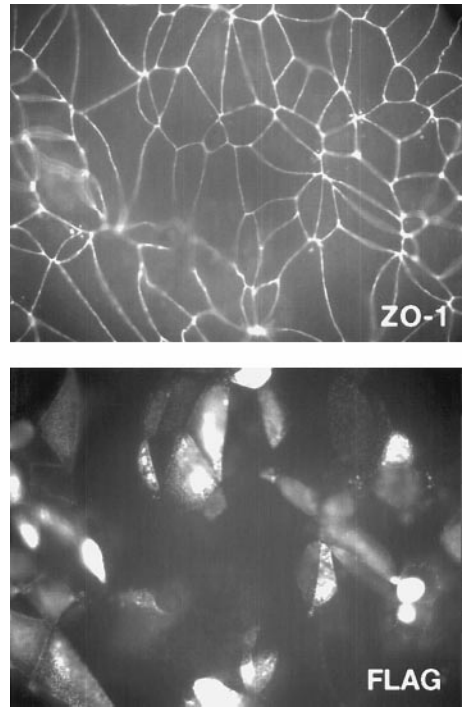

Fig. 3. M2–901/CFTR is expressed at the apical surface in FSK-stimulated polarized MDCK cells. Filter-grown MDCK cells were mock infected or infected with AV-M2–901 at an MOI of 50. Cells were treated with 10 μM FSK for 20 min at 37°C, rapidly chilled, processed live for indirect immunofluorescence to detect surface CFTR using the FLAG antibody (*bottom*), and then fixed, permeabilized, and labeled using anti-ZO-1 antibody to detect tight junctions (*top*). Images were taken at the same focal plane.

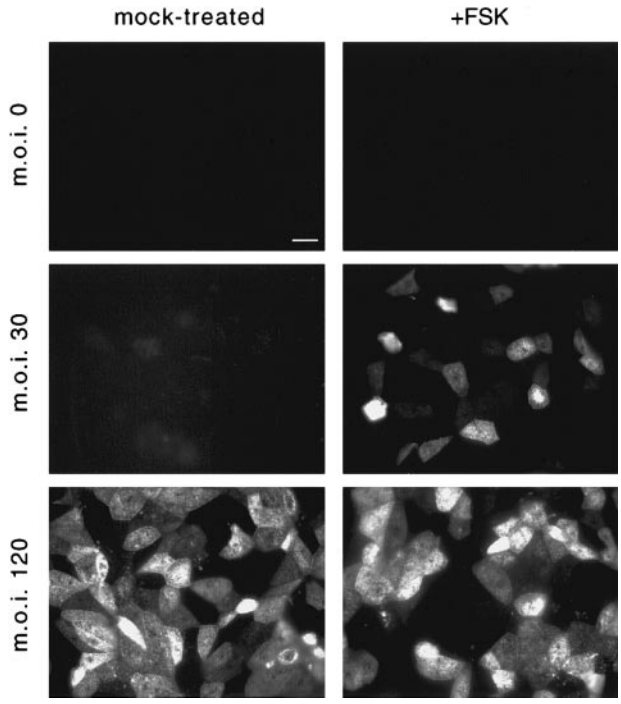

Fig. 4. FSK stimulation of M2–901/CFTR membrane insertion in polarized MDCK cells is expression-level dependent. Filter-grown MDCK cells were mock infected or infected with AV-M2–901 at an MOI of 30 or 120. The following day, cells were treated with 10 μM FSK for 20 min at 37°C. Cells were rapidly chilled to 0°C and processed live to detect surface CFTR using the FLAG antibody. Images were taken at identical exposures. The small unstained area in the center of heavily labeled cells is where the cilium on each cell is anchored. Scale bar: 10 μm.

larized MDCK cells infected at low MOI with AV-M2–901 (Fig. 5). A dramatic redistribution of M2–901/CFTR was observed in cells stimulated with FSK compared with mock-stimulated cells. In unstimulated cells, M2–901/CFTR was concentrated in a heterogeneous population of tubules and vesicles near the cell surface; by contrast, most of the M2–901/CFTR in FSK-stimulated cells was found at the PM. Interestingly, surface M2–901/CFTR in FSK-stimulated cells tended to be concentrated at the tips of membrane projections on the cell surface; these might represent membrane exocytosed during FSK stimulation. Quantitation of the distribution of M2–901/CFTR in two independent experiments revealed a statistically significant increase in surface M2–901/CFTR in FSK-stimulated cells at low MOI (Table 1). By contrast, FSK treatment of cells infected at high MOI (100) had only a small and not statistically significant effect on surface M2–901/CFTR. Although the degree of increase in surface M2–901/CFTR observed upon FSK stimulation of cells infected at low MOI was similar in the two experiments (~2.0- vs. 2.8-fold), the overall distribution of M2–901/CFTR after FSK stimulation was variable (between 20 and 80% of total M2–901/CFTR present at the PM). This was not unexpected given the variability in surface staining we detected in the fluorescence experiments. Overall, the results clearly support a model for cAMP-stimulated insertion of M2–901/CFTR into the apical PM of MDCK cells.

DISCUSSION

We have developed a replication-defective recombinant adenovirus expressing epitope-tagged CFTR and used it to study membrane trafficking of this ion channel in response to FSK stimulation. Infection of polarized MDCK cells obtained from two independent sources with the adenovirus did not affect the morphology of the cells and resulted in expression of functional cAMP-stimulated chloride channel conductance. At low MOI (30–50), little M2–901/CFTR was detected on the PM of unstimulated, nonpermeabilized cells by indirect immunofluorescence, whereas FSK stimulation caused a dramatic increase in the amount of cell surface M2–901/CFTR. By contrast, at higher MOI (>100), considerable M2–901/CFTR was detected at the PM of unstimulated cells, and no further increase could be detected by indirect immunofluorescence upon FSK addition. Immunoelectron microscopy showed that M2–901/CFTR expressed at low levels in unstimulated cells was primarily found in subapical vesicles, whereas M2–901/CFTR levels at the PM were increased in FSK-treated cells. These results demonstrate that CFTR insertion in the apical PM of MDCK cells is regulated by cAMP stimulation.

Our observations using indirect immunofluorescence suggest that, at low expression levels, CFTR may be concentrated primarily in a subapical compartment whose fusion with the membrane is regulated by increased cAMP levels. There are numerous other examples of transporters that undergo regulated trafficking, including the insulin-responsive glucose transporter GLUT-4, the vasopressin-sensitive water channel aquaporin-2, the renal epithelial proton pump, and the potassium-dependent proton pump of gastric parietal cells (3, 7, 12, 34). At higher expression levels, the CFTR-containing regulated compartment might be saturated, resulting in CFTR "leakage" into other compartments as well as the PM. Elevated levels of cAMP are also known to stimulate the rate of apical membrane insertion of proteins from the *trans*-Golgi network and apical recycling endosomes in MDCK II cells. For example, apical delivery of the membrane protein influenza hemagglutinin and apical secretion of the endogenous gp80 complex of MDCK cells is markedly stimulated by increased cAMP levels (2, 8, 27). In addition, the rate of basolateral-to-apical transcytosis of the polymeric immunoglobulin receptor in stably transfected MDCK cells is enhanced in cells treated with FSK and IBMX; the cAMP-stimulated step in this pathway is the transport of the receptor from a subapical endocytic compartment to the apical surface (8). Thus M2–901/CFTR present in these compartments should also be inserted in the apical PM upon FSK stimulation. This might explain why we detected a slight cAMP-dependent increase in surface expression of CFTR expressed at high levels using immunoelectron microscopy.

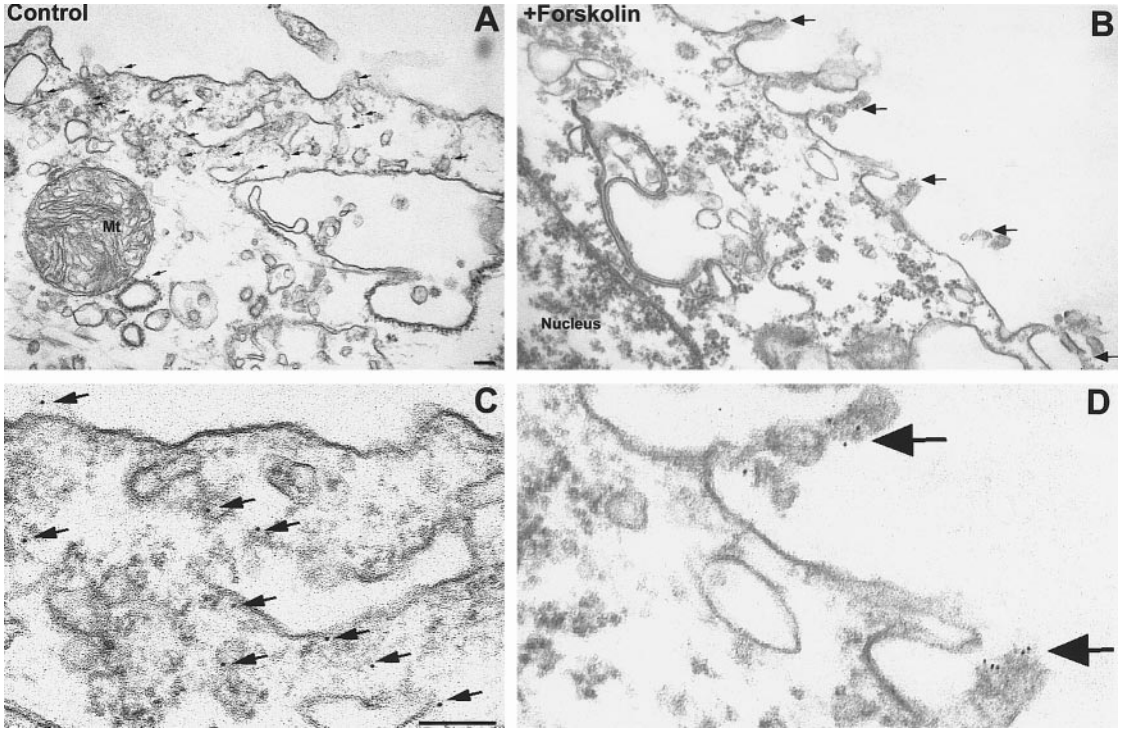

Fig. 5. Immunoelectron microscopy of M2–901/CFTR in untreated and FSK-stimulated MDCK cells. Filter-grown MDCK cells were infected with AV-M2–901 at an MOI of 50. The following day, cells were mock treated or treated with 10 μM FSK for 20 min at 37°C and then rapidly chilled. Cells were processed for immunoelectron microscopy using the anti-carboxy terminal antibody directed against CFTR as described in EXPERIMENTAL PROCEDURES. Representative images of mock-treated (*A*) or FSK-treated (*B*) cells labeled with gold particles (arrows) are shown. Higher magnification views of the cells in *A* and *B* are shown in *C* and *D*, respectively. No labeling was observed over nuclei or mitochondria (Mt). Scale bar: 100 nm.

Although cAMP elevation can regulate membrane trafficking events in some cells (including MDCK) in the absence of CFTR, there are several systems in which CFTR is required for cAMP-dependent membrane trafficking (1, 32, 35). For example, cAMP causes a dramatic increase in membrane exocytosis in oocytes that express CFTR but not in water-injected oocytes (35). Thus it appears that expression of CFTR can create a regulated compartment in some cell types. In addition to its regulation of membrane trafficking, CFTR is also known to regulate the activity of other channels and transporters (5, 16, 18, 26, 30, 33). Second messenger-mediated control of CFTR localization could thus provide an added level of cellular control

Table 1. *Quantitation of M2-901/CFTR distribution in FSK- and mock-stimulated MDCK cells*

	No. of Cells Counted	Gold at Surface	Total Gold Particles Counted	% At PM	Degree of FSK-stimulated Increase at Cell Surface
			Experiment 1		
MOI 50					
+FSK	16	370	453	81.6	2.84*
−FSK	14	84	293	28.7	
			Experiment 2		
MOI 30					
+FSK	9	54	288	18.8	2.04†
−FSK	11	24	260	9.2	
MOI 100					
+FSK	26	77	301	25.6	1.35
−FSK	14	60	318	18.9	

Immunogold labeling of forskolin (FSK)- and mock-stimulated cells infected with adenovirus (AV)-M2–901 at the indicated multiplicity of infection (MOI) was performed as described in EXPERIMENTAL PROCEDURES. *Experiment 1* was performed using standard Madin-Darby canine kidney (MDCK) II cells, whereas *experiment 2* was performed using the CCL subclone. The samples were blinded, and photographs were taken of at least 9 cells from each sample. The number of gold particles on the cell surface and inside were counted, and the % of particles at the plasma membrane (PM) was calculated. CFTR, cystic fibrosis transmembrane conductance regulator. *$P < 0.0001$. †$P = 0.04$.

over CFTR activity, membrane trafficking, and the activity of other channels and transporters.

Our results differ from those of Moyer et al. (23), who concluded that, in MDCK I cells, cAMP stimulation does not increase the level of cell surface CFTR tagged at the amino terminus with GFP. Several reasons might explain the differences between our results. First, the GFP-tagged construct was presumably expressed at relatively high levels, as the brightest cells from each transfection were selected for expansion. In these cells, a high fraction (>50% by our estimate) of GFP-CFTR was already present at the surface of unstimulated cells. By contrast, at low expression levels, we found almost no M2–901/CFTR at the PM of unstimulated MDCK II cells; however, considerable cell surface expression was detected in unstimulated cells expressing higher levels of M2–901/CFTR (Fig. 4). In addition, unlike MDCK II cells, which do not express detectable functional CFTR (Fig. 2), polarized MDCK I cells express significant levels of this channel (20). Thus it is possible that even low levels of expression of the heterologous GFP-tagged construct could saturate the system. In support of this hypothesis, the short-circuit current of unstimulated GFP-CFTR-expressing cells was nearly 20-fold higher than cAMP-stimulated untransfected MDCK I cells. To our knowledge, the effect of FSK on apical membrane insertion of newly synthesized and transcytosed proteins in MDCK I cells has not been investigated. Second, it is possible that the GFP-tagged construct expressed in MDCK cells is not regulated in the same manner as wild-type or M2-tagged CFTR. Recent experiments have demonstrated that syntaxin 1A binds to the amino terminus of CFTR (25). Syntaxin 1A binding inhibits cAMP-stimulated channel activity in *Xenopus* oocytes (possibly by inhibiting the membrane insertion of CFTR; see Refs. 24 and 28) and in the colonic epithelial cell line T84 (24). Finally, it is possible that the differences we observed are due to differences in the cell types used. One possibility is that MDCK II cells, which do not express endogenous CFTR, might lack specialized machinery required for PM insertion of CFTR. We consider this possibility unlikely, as cell surface delivery is believed to be the default trafficking route for membrane proteins. However, there is substantial evidence to suggest that CFTR trafficking is cell type dependent. For example, Loffing et al. (19) demonstrated that localization of endogenous CFTR in the airway cell line Calu-3 appears to be unaffected by cAMP stimulators. Preliminary data from our laboratory also suggest that FSK does not stimulate insertion of M2–901/CFTR in Calu-3 cells infected with AV-M2–901, even at low MOI; however, it should be noted that these cells already express considerable levels of endogenous CFTR (Weisz, unpublished observations). In addition, Hug et al. (15) reported that activation of CFTR in stably transfected Chinese hamster ovary cells occurred in the absence of exocytosis. By contrast, FSK stimulation caused a quantitative increase in surface M2–901/CFTR expressed in HeLa cells (14). Moreover, arginine vasotocin stimulation causes microtubule-dependent insertion of subcellular CFTR into the apical PM of A6 cells (a model for the kidney collecting duct; see Ref. 22), suggesting that at least this part of the kidney can regulate membrane insertion of CFTR. MDCK type II cells are thought to be derived from the distal nephron, whereas the origin of MDCK I cells is still debated (9, 29). Given the divergent physiological functions of the kidney, it is plausible that CFTR trafficking could be differentially regulated by cells from different regions of this organ.

It is clear that the amount of CFTR expressed in a given tissue can have dramatic consequences on organ physiology and development as well as susceptibility to disease. For example, mice heterozygous for wild-type CFTR are resistant to cholera toxin compared with normal mice (6). Furthermore, a threshold level of CFTR expression may be important for proper development of the vas deferens (4). However, too much CFTR may be problematic, as a recent report suggests that overexpression of CFTR in several cell lines results in loss of its ability to regulate other ion channels (21). Our data further emphasize the importance of evaluating the effect of protein expression level on CFTR trafficking, function, and regulation in epithelial cells.

We thank Frances Shagas for help with the immunoelectron microscopy, Genzyme for the recombinant adenovirus encoding wild-type CFTR, and Drs. Randy Brown and William J. Welch for the antibody directed against the R domain of CFTR.

This study was supported by grants from the Cystic Fibrosis Foundation (to O. A. Weisz), National Institute of Diabetes and Digestive and Kidney Diseases Grants DK-54407 (to O. A. Weisz), DK-44935 (to P. D. Robbins), and DK-50829 (to R. A. Frizzell), and the American Lung Association (to M. Howard).

REFERENCES

1. **Bradbury NA, Jilling T, Berta G, Sorscher EJ, Bridges RJ, and Kirk KL.** Regulation of plasma membrane recycling by CFTR. *Science* 256: 530–532, 1992.
2. **Brignoni M, Pignataro OP, Rodriguez ML, Alvarez A, Vega-Salas DE, Rodriguez-Boulan E, and Salas PJI.** Cyclic AMP modulates the rate of "constitutive" exocytosis of apical membrane proteins in Madin-Darby canine kidney cells. *J Cell Sci* 108: 1931–1943, 1985.
3. **Cannon C, van Adelsberg J, Kelly S, and Al-Awqati Q.** Carbon-dioxide-induced exocytotic insertion of H^+ pumps in turtle-bladder luminal membrane: role of cell pH and calcium. *Nature* 314: 443–446, 1985.
4. **De Braekeleer M and Ferec C.** Mutations in the cystic fibrosis gene in men with congenital bilateral absence of the vas deferens. *Mol Human Reprod* 2: 669–677, 1996.
5. **Egan M, Flotte TR, Afione S, Solow R, Zeitlin PL, Carter BJ, and Guggino WB.** Defective regulation of outwardly rectifying Cl^- channels by protein kinase A corrected by insertion of CFTR. *Nature* 358: 581–584, 1992.
6. **Gabriel SE, Brigman KN, Koller BH, Boucher RC, and Stutts MJ.** Cystic fibrosis heterozygote resistance to cholera toxin in the cystic fibrosis mouse model. *Science* 266: 107–109, 1994.
7. **Handler JS.** Antidiuretic hormone moves membranes. *Am J Physiol Renal Fluid Electrolyte Physiol* 255: F375–F382, 1988.
8. **Hansen SH and Casanova JE.** Gsα stimulates transcytosis and apical secretion in MDCK cells through cAMP and protein kinase A. *J Cell Biol* 126: 677–687, 1994.
9. **Hansson GC, Simons K, and van Meer G.** Two strains of the Madin-Darby canine kidney (MDCK) cell line have distinct glycosphingolipid compositions. *EMBO J* 5: 483–489, 1986.

10. **Hardy S, Kitamura M, Harris-Stansil T, Dai Y, and Phipps ML.** Construction of adenovirus vectors through Cre-*lox* recombination. *J Virol* 71: 1842–1849, 1997.
11. **Henkel JR, Apodaca G, Altschuler Y, Hardy S, and Weisz OA.** Selective perturbation of apical membrane traffic by expression of influenza virus M2, an acid-activated ion channel, in polarized Madin-Darby canine kidney cells. *Mol Biol Cell* 8: 2477–2490, 1998.
12. **Hirst BH and Forte JG.** Redistribution and characterization of (H^+,K)-ATPase membranes from resting and stimulated gastric parietal cells. *Biochem J* 231: 641–649, 1985.
13. **Howard M, DuVall MD, Devor DC, Dong J, Henze K, and Frizzell RA.** Epitope tagging permits cell surface detection of functional CFTR. *Am J Physiol Cell Physiol* 269: C1565–C1576, 1995.
14. **Howard M, Jilling T, DuVall M, and Frizzell RA.** cAMP-regulated trafficking of epitope-tagged CFTR. *Kidney Int* 49: 1642–1648, 1996.
15. **Hug MJ, Thiele IE, and Greger R.** The role of exocytosis in the activation of the chloride conductance in Chinese hamster ovary cells (CHO) stably expressing CFTR. *Pflügers Arch* 434: 779–784, 1997.
16. **Ismailov II, Awayda MS, Jojov B, Berdiev BK, Fuller CM, Dedman JR, Kaetzel MA, and Benos DJ.** Regulation of epithelial sodium channels by the cystic fibrosis transmembrane conductance regulator. *J Biol Chem* 271: 4725–4732, 1996.
17. **Jiang X, Hill WG, Pilewski JM, and Weisz OA.** Glycosylation differences between a cystic fibrosis and rescued airway cell line are not CFTR dependent. *Am J Physiol Lung Cell Mol Physiol* 273: L913–L920, 1997.
18. **Jojov B, Ismailov II, Berdiev BK, Fuller CM, Sorscher EJ, Dedman JR, Kaetzel MA, and Benos DJ.** Interaction between cystic fibrosis transmembrane conductance regulator and outwardly rectified chloride channels. *J Biol Chem* 270: 29194–29200, 1995.
19. **Loffing J, Moyer BD, McCoy D, and Stanton BA.** Exocytosis is not involved in activation of Cl^- secretion via CFTR in Calu-3 airway epithelial cells. *Am J Physiol Cell Physiol* 275: C913–C920, 1998.
20. **Mohamed A, Ferguson D, Seibert FS, Cai H, Kartner N, Grinstein S, Riordan JR, and Lukacs GL.** Functional expression and apical localization of the cystic fibrosis transmembrane conductance regulator in MDCK I cells. *Biochem J* 322: 259–265, 1997.
21. **Mohammad-Panah R, Demolombe S, Riochet D, Leblais V, Loussouarn G, Pollard H, Baro I, and Escande D.** Hyperexpression of recombinant CFTR in heterologous cells alters its physiological properties. *Am J Physiol Cell Physiol* 274: C310–C318, 1998.
22. **Morris RG, Tousson A, Benos DJ, and Schafer JA.** Microtubule disruption inhibits AVT-stimulated Cl^- secretion but not Na^+ reabsorption in A6 cells. *Am J Physiol Renal Physiol* 274: F300–F314, 1998.
23. **Moyer BD, Loffing J, Schwiebert EM, Loffing-Cueni D, Halpin PA, Karlson KH, Ismailov II, Guggino WB, Langford GM, and Stanton BA.** Membrane trafficking of the cystic fibrosis gene product, cystic fibrosis transmembrane conductance regulator, tagged with green fluorescent protein in Madin-Darby canine kidney cells. *J Biol Chem* 273: 21759–21768, 1998.
24. **Naren AP, Nelson DJ, Xie W, Jovov B, Pevsner J, Bennett MK, Benos DJ, Quick MW, and Kirk KL.** Regulation of CFTR chloride channels by syntaxin and Munc18 isoforms. *Nature* 390: 302–305, 1997.
25. **Naren AP, Quick MW, Collawn JF, Nelson DJ, and Kirk KL.** Syntaxin 1A inhibits CFTR chloride channels by means of domain-specific protein-protein interactions. *Proc Natl Acad Sci USA* 95: 10972–10977, 1998.
26. **Pasyk EA and Foskett JK.** Cystic fibrosis transmembrane conductance regulator-associated ATP and adenosine 3′-phosphate 5′-phosphosulfate channels in endoplasmic reticulum and plasma membrane. *J Biol Chem* 272: 7746–7751, 1997.
27. **Pimplikar SW and Simons K.** Activators of protein kinase A stimulate apical but not basolateral transport in epithelial Madin-Darby canine kidney cells. *J Biol Chem* 269: 19054–19059, 1994.
28. **Qi JJ, Peters KW, Watkins SC, and Frizzell RA.** Syntaxin 1A inhibits regulated CFTR trafficking. *Pediatr Pulmonol Suppl* 17: 201–202, 1998.
29. **Richardson JC, Scalera V, and Simmons NL.** Identification of two strains of MDCK cells which resemble separate nephron tubule segments. *Biochim Biophys Acta* 673: 26–36, 1981.
30. **Ruknudin A, Shulze DH, Sullivan SK, Lederer WJ, and Welling PA.** Novel subunit composition of a renal epithelial K_{ATP} channel. *J Biol Chem* 273: 14165–14171, 1998.
31. **Schultz BD, Takahashi A, Liu C, Frizzell RA, and Howard M.** FLAG epitope positioned in an external loop preserves normal biophysical properties of CFTR. *Am J Physiol Cell Physiol* 273: C2080–C2089, 1997.
32. **Schwiebert EM, Gesek F, Ercolani L, Wjasow C, Gruenert DC, Karlson K, and Stanton BA.** Heterotrimeric G proteins, vesicle trafficking, and CFTR Cl^- channels. *Am J Physiol Cell Physiol* 267: C272–C281, 1994.
33. **Stutts MJ, Canessa CM, Olsen JC, Hamrick M, Cohn JA, Rossier BC, and Boucher RC.** CFTR as a cAMP-dependent regulator of sodium channels. *Science* 269: 847–850, 1995.
34. **Suzuki K and Kono T.** Evidence that insulin causes translocation of glucose transport activity to the plasma membrane from an intracellular storage site. *Proc Natl Acad Sci USA* 77: 2542–2545, 1985.
35. **Takahashi A, Watkins SC, Howard M, and Frizzell RA.** CFTR-dependent membrane insertion is linked to stimulation of the CFTR chloride conductance. *Am J Physiol Cell Physiol* 271: C1887–C1894, 1996.